# Delivery of Peptides to the Blood and Brain after Oral Uptake of Quaternary Ammonium Palmitoyl Glycol Chitosan Nanoparticles

**ARTICLE** *in* MOLECULAR PHARMACEUTICS · MAY 2012

Impact Factor: 4.38 · DOI: 10.1021/mp300068j · Source: PubMed



**6 AUTHORS**, INCLUDING:

Aikaterini Lalatsa
University of Portsmouth
**16** PUBLICATIONS **209** CITATIONS
SEE PROFILE

Natalie Laura Garrett
University of Exeter
**21** PUBLICATIONS **208** CITATIONS
SEE PROFILE

J. Moger
University of Exeter
**57** PUBLICATIONS **1,272** CITATIONS
SEE PROFILE

molecular pharmaceutics

Article

pubs.acs.org/molecularpharmaceutics

# Delivery of Peptides to the Blood and Brain after Oral Uptake of Quaternary Ammonium Palmitoyl Glycol Chitosan Nanoparticles

A. Lalatsa,[†] N. L. Garrett,[‡] T. Ferrarelli,[†,§] J. Moger,[‡] A. G. Schätzlein,[†,∥] and I. F. Uchegbu*[,†,∥]

[†]UCL School of Pharmacy, University of London, 29-39 Brunswick Square, London, U.K., WC1N 1AX

[‡]School of Physics, University of Exeter, Stocker Road, Exeter, U.K., EX4 4QL

[∥]Nanomerics Ltd., 14 Approach Road, St. Albans, Hertfordshire, U.K., AL1 1SR

Supporting Information

**ABSTRACT:** The clinical development of therapeutic peptides has been restricted to peptides for non-CNS diseases and parenteral dosage forms due to the poor permeation of peptides across the gastrointestinal mucosa and the blood−brain barrier. Quaternary ammonium palmitoyl glycol chitosan (GCPQ) nanoparticles facilitate the brain delivery of orally administered peptides such as leucine[5]-enkephalin, and here we examine the mechanism of GCPQ facilitated oral peptide absorption and brain delivery. By analyzing the oral biodistribution of radiolabeled GCPQ nanoparticles, the oral biodistribution of the model peptide leucine[5]-enkephalin and coherent anti-Stokes Raman scattering microscopy tissue images after an oral dose of deuterated GCPQ nanoparticles, we have established a number of facts. Although 85−90% of orally administered GCPQ nanoparticles are not absorbed from the gastrointestinal tract, a peak level of 2−3% of the oral GCPQ dose is detected in the blood 30 min after dosing, and these GCPQ particles appear to transport the peptides to the blood. Additionally, although peptide loaded nanoparticles from low (6 kDa) and high (50 kDa) molecular weight GCPQ are taken up by enterocytes, polymer particles with a polymer molecular weight greater than 6 kDa are required to facilitate peptide delivery to the brain after oral administration. By examining our current and previous data, we conclude that GCPQ particles facilitate oral peptide absorption by protecting the peptide from gastrointestinal degradation, adhering to the mucus to increase the drug gut residence time and transporting GCPQ associated peptide across the enterocytes and to the systemic circulation, enabling the GCPQ stabilized peptide to be transported to the brain. Orally administered GCPQ particles are also circulated from the gastrointestinal tract to the liver and onward to the gall bladder, presumably for final transport back to the gastrointestinal tract.

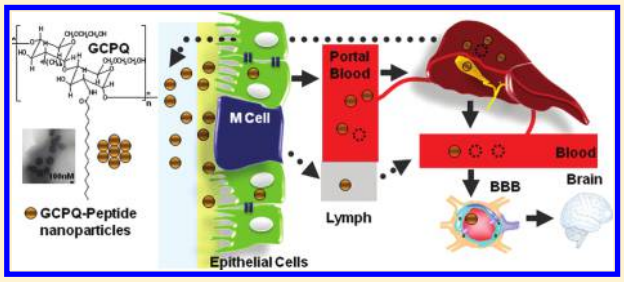


**KEYWORDS:** *chitosan nanoparticles, nanoparticle oral uptake, chitosan amphiphiles, oral peptide delivery, quaternary ammonium palmitoyl glycol chitosan, GCPQ, molecular weight, biodistribution, leucine[5]-enkephalin, CARS microscopy*

## INTRODUCTION

Recent advances in chemical synthesis methodologies and recombinant DNA technology allow for the production of large quantities of structurally diverse therapeutic peptides and proteins (antibodies, hormones and vaccines). Although new biopharmaceuticals for more than 100 diseases such as cancer, infectious diseases and autoimmune diseases are currently in human clinical trials or under review by the Food and Drug Administration,[1] the clinical development of these drugs has been restricted due to their poor permeation across biological barriers such as the gastrointestinal tract (GIT) epithelium[2,3] and the blood−brain barrier (BBB).[4] In essence the formulation of biopharmaceuticals still remains a challenge for the pharmaceutical industry. Parenteral administration of pharmaceutical peptides or proteins is usual, due to their low oral bioavailability (<1%). However, parenteral routes are expensive and invasive, especially for chronic conditions.

Quaternary ammonium palmitoyl glycol chitosan (GCPQ) is an amphiphilic polymer which assembles into stable nanoparticles that increase the transport of hydrophilic and hydrophobic drugs across the GIT epithelium,[5,6] BBB[5,7] and cornea.[7] While we understand the mechanisms by which GCPQ nanoparticles enhance the oral delivery of hydrophobic drugs,[6] we are uncertain as to the mechanism by which GCPQ nanoparticles enhance the oral delivery of hydrophilic biomacromolecules, such as peptides.[5] In the case of hydrophobic drugs, GCPQ nanoparticles form highly stable self-assemblies encapsulating such drugs,[6,7] which (a) provide a large potential diffusion gradient by encapsulating drugs at a high particle concentration, (b) provide a high surface area reservoir for faster drug dissolution, and (c) promote drug epithelial transport through nanoparticle adhesion to and invasion into the mucus, allowing prolonged intimate contact

**Received:** February 7, 2012
**Revised:** April 20, 2012
**Accepted:** May 9, 2012
**Published:** May 9, 2012

  

between the loaded particles and the absorptive enterocytes of the GIT.[6]

We hypothesized that GCPQ molecular weight and particle oral absorption would play a role in the mechanism by which GCPQ particles enhanced the oral delivery of hydrophilic peptides. We thus determined the biodistribution of radiolabeled orally administered GCPQ particles, determined the tissue levels of the model peptide leucine[5]-enkephalin following its oral administration in GCPQ–leucine[5]-enkephalin particles, and determined the plasma stability of GCPQ–leucine[5]-enkephalin particles. A multimodal imaging strategy was used to image the fate of orally administered deuterated GCPQ particles without chemical perturbation. Specifically, we utilized a combination of coherent anti-Stokes Raman scattering (CARS) microscopy, two-photon autofluorescence (TPF), and second harmonic generation (SHG) to provide chemically specific contrast of nanoparticles, cells, and extracellular matrix elements.[8,9]

The experimental data so obtained allowed us to establish some facts about the mechanism of oral peptide delivery: GCPQ particles facilitate oral absorption by being transported into the blood. Furthermore, such particles need to have a GCPQ molecular weight in excess of 6 kDa in order for orally administered GCPQ-peptide particles to facilitate subsequent delivery of the peptides to the brain. Drawing on our current and earlier findings, we are thus able to draw broad conclusions about the mechanism of action of GCPQ in so far as it relates to the oral delivery of hydrophilic peptides.

## EXPERIMENTAL SECTION

**Materials.** All reagents and chemicals were obtained from Sigma Aldrich Chemical Co. (Poole, U.K.) and solvents and acids from Fisher Scientific (Loughborough, U.K.) or VWR (Lutterworth, U.K.) unless otherwise stated. Visking seamless cellulose dialysis membranes were purchased from Medicell International Ltd. (London, U.K.). Deuterium oxide and methanol-$d_6$ were obtained from Cambridge Isotope Laboratories, Inc. (via Goss Scientific Instruments, Cheshire, U.K.), and the Bolton Hunter reagent was obtained from Perkin-Elmer, Inc. (Cambridge, U.K.). Leucine[5]-enkephalin was obtained from Peptisyntha Inc. (Torrance, U.S.A.). The radioimmunoassay kits for leucine[5]-enkephalin were obtained from Bachem, Ltd. (S-2118, St Helens, U.K.). All reagents and chemicals were used without further purification and were ≥98% pure.

**Synthesis and Characterization of Chitosan Amphiphiles.** The acid degradation of glycol chitosan (GC) was carried out as described previously.[10] Briefly, GC (5 g) was dissolved in hydrochloric acid (4 M, 380 mL) incubated at 50 °C for 2, 24, or 48 h and purified by exhaustive dialysis. The molecular weight of the product was controlled by the degradation time as increasing the acid degradation time leads to a decrease in polymer molecular weight.[10] The product was purified by exhaustive dialysis (Visking tubing, molecular weight cutoff = 12–14 kDa for the 2 h and 24 h degraded polymers or Visking tubing, molecular weight cutoff = 3.5 kDa for the 48 h degraded polymer) and the products freeze-dried to give GC50 (degradation time = 2 h), GC14 (degradation time = 24 h) and GC10 (degradation time = 48 h).

To prepare GC6, GC48 (1 g) was re-degraded by dissolving in hydrochloric acid (10 M, 76 mL) and stirred in a preheated oil bath at 50 °C under reflux conditions. To avoid oxidation, the reaction mixture was purged with $N_2$ and the reaction was protected from light. After 9 h the reaction was stopped and the product was removed. The solution was diluted with Millipore double-deionized water (<18 Ω) to a final acid concentration of <4 M. The product was purified by exhaustive dialysis (3.5 kDa) against deionized water (5 L) with six changes over 24 h. The dialysate was subsequently freeze-dried, and the product was recovered as a white-colored cotton-wool-like material (GC6).

The molecular weights of the GC and GCPQ polymers were determined using gel permeation chromatography and multi-angle laser light scattering (Table SI-1 in the Supporting Information and Table 1) using a Wyatt gel permeation chromatography–multi-angle laser light scattering instrument (GPC-MALLS) equipped with Dawn Heleos II MALLS detector (120 mW solid-state laser operating at $\lambda$ = 658 nm), Optilab rEX interferometric refractometer (flow cell: 7.4 μL, $\lambda$ = 658 nm) and quasielastic light scattering (QELS) detectors (Wyatt Technology Corporation, Santa Barbara, CA, USA). The mobile phase used was an acetate buffer (0.3 M anhydrous sodium acetate, 0.2 M glacial acetic acid, pH = 4.5) for GC and a mixture of acetate buffer and methanol (35: 65 v/v) for GCPQ. Filtered samples (0.2 μm, PES, Millipore Millex-HA, 100 μL) were injected using an Agilent 1200 series autosampler (Agilent Instruments, Stockport, U.K.) on to a POLYSEP-GFC-P guard column (35 × 7.8 mm, Phenomenex, Macclesfied, U.K.) attached to a POLYSEP-GFC-P 4000 column (300 × 7.8 mm, exclusion limit for PEG = 200 kDa, Phenomenex) at a loading concentration of 5 mg $mL^{-1}$. Measurements in triplicate were performed at room temperature with a mobile phase flow rate of 0.9 mL $min^{-1}$ (Agilent 1200 series isocratic pump attached to an Agilent 1200 series degasser). The data were processed using ASTRA for Windows version 5.3.4.14 software (Wyatt Technology Corporation). Toluene and BSA were used for Dawn HELEOS II MALLS calibration and normalization, respectively.

The syntheses of GCPQ6, GCPQ10, GCPQ14 and GCPQ50 from GC6, GC10, GC14 and GC50 respectively were carried out as previously described.[6] Radiolabeled[5] and deuterated[8,9] GCPQ were synthesized and characterized as previously described. The specific radioactivity of radiolabeled GCPQ was 0.16 ± 0.01 μCi $mg^{-1}$, containing less than 2% free iodine as quantified by TLC after purification by exhaustive dialysis (Visking tubing, molecular weight cutoff = 3.5 kDa, 12 by 3 L changes over 18 h). The molecular weight of the deuterated GCPQ (dGCPQ) polymers was analyzed using GPC-MALLS as described above, and the FT-IR spectra were obtained using a using a PerkinElmer Spectrum 100 FTIR spectrometer equipped with a Universal attenuated total reflectance (UATR) accessory and a zinc selenide crystal (4000 to 650 $cm^{-1}$) and Spectrum FT-IR software (maximum resolution is 1 $cm^{-1}$) (Table 1).

**Manufacture and Characterization of GCPQ Particles.** GCPQ nanoparticles were prepared by probe sonication (Soniprep 150 Instruments, MSE, U.K.) of aqueous dispersions of GCPQ.[6] Particles were imaged by transmission electron microscopy,[6] and the enthalpy of demicellization of the various GCPQ aggregates (and in turn their critical micellar concentrations) was determined using a VP-ITC microcalorimeter (MicroCal, LLC, Northampton, MA, USA).[6]

The kinematic viscosity of GCPQ dispersions was measured using an automated capillary viscometer (range 0.3–10 mPa.s, AMVn automated microviscometer, Anton Paar, Austria). Freshly prepared and degassed GCPQ aqueous dispersions

Table 1. Chitosan Amphiphiles (GCPQ) Polymer Sample Characteristics

| polymer | yield (%) | $M_w$ (Da) | $M_n$ (Da) | $M_w/M_n$ | FTIR signal ($cm^{-1}$) for C−D stretch | d$n$/dc (mL $g^{-1}$) | kinematic viscosity (mPa·S) 20 °C, 6.75 mg $mL^{-1}$ | CMC ($\mu$M) | P (% − per 100 monomers) | Q (% − per 100 monomers) | A (% − per 100 monomers) |
|---|---|---|---|---|---|---|---|---|---|---|---|
| GCPQ6 | 48.1 | 6,019 ± 296 | 5,416 ± 234 | 1.11 ± 0.027 | n/a | 0.163 ± 0.002 | 0.946 ± 0.002 | 14 | 19.8 ± 0.4 | 10.8 ± 1.8 | 0.1 ± 0.02 |
| GCPQ10 | 45.3 | 11,732 ± 949 | 11,075 ± 1,138 | 1.06 ± 0.023 | n/a | 0.149 ± 0.009 | 1.015 ± 0.001 | 14 | 17.4 ± 1.3 | 11.8 ± 1.8 | 0.8 ± 0.29 |
| GCPQ14 | 44.7 | 16,386 ± 2726 | 12,815 ± 3,995 | 1.32 ± 0.240 | n/a | 0.191 ± 0.043 | 1.413 ± 0.003 | 19[a] | 19.0 ± 1.3 | 11.4 ± 3.6 | 2.0 ± 0.44 |
| GCPQ50 | 52.1 | 58,646 ± 2621 | 40,533 ± 7,895 | 1.48 ± 0.262 | n/a | 0.140 ± 0.006 | 4.051 ± 0.072 | 13 | 11.1 ± 0.6 | 10.9 ± 2.2 | 10.1 ± 1.3 |
| DGCPQ6 | 52.5 | 9,110 | 8,567 | 1.06 | 2101−2203 | 0.143 ± 0.004 | nd | nd | nd | nd | nd |
| DGCPQ10 | 52.9 | 11,970 | 13,990 | 1.17 | 2094−2205 | 0.135 ± 0.002 | nd | nd | nd | nd | nd |
| DGCPQ50 | 54.0 | 75,410 | 57,250 | 1.32 | 2096−2204 | 0.109 ± 0.00 | nd | nd | nd | nd | nd |

[a]Data taken from ref 6. Key: P, palmitoylation; Q, quaternization; A, acetylation; n/a, not applicable; nd, not determined.

(6.75 mg $mL^{-1}$, 400 $\mu$L) were analyzed at 20 °C. Measurements were carried out at a fixed angle of 30°, and the viscosity of water at 25 °C was determined to be 0.9614 mPa·s (angle = 30°). The dynamic viscosity was derived from the kinematic viscosity.

GCPQ−leucine$^5$-enkephalin formulations were prepared in sterile water for injection (pH 5.5) by vortexing a mixture of GCPQ (75 mg $mL^{-1}$) and leucine$^5$-enkephalin (15 mg $mL^{-1}$), followed by probe sonication (MSE Soniprep 150, MSE, U.K., with the instrument set at 75% of its maximum output) for 15 min on ice. The formulations were left overnight in the refrigerator (2−8 °C). After 10−12 h, the formulations were sonicated for a further 15 min.

**Encapsulation Studies.** Ultracentrifugation was used to characterize the loading. Freshly prepared nanoparticle formulations (200 $\mu$L, 4 mg $mL^{-1}$ of leucine$^5$-enkephalin and 10.4 mg $mL^{-1}$ of GCPQ in 0.9% NaCl) were centrifuged in polyallomer tubes (169000$g$, 45 min at 4 °C) using a Beckman Coulter Optima MAX-E ultracentrifuge. Immediately after centrifugation, the supernatant and pellet were diluted/resuspended with mobile phase and then analyzed via HPLC. The pellet was resuspended in mobile phase and analyzed via HPLC. Two reverse phase Phenomenex Onyx Monolithic C18 columns (5 $\mu$m, 4.6 × 100 mm) connected in series with a guard column (5 $\mu$m, 4.6 × 10 mm) were used on an Agilent 1200 series HPLC (Agilent Technologies, Wokingham, U.K.) equipped with a quaternary pump, degasser, autosampler and a UV detector. The mobile phase used consisted of water:-acetonitrile (82:18 v/v) with 0.02% TFA. The flow rate was set at 1.5 mL $min^{-1}$, the temperature at 30 °C with an injection volume of 40 $\mu$L. Agilent ChemStation software was used for data analysis, the retention time was 9.6 min for leucine$^5$-enkephalin and a linear calibration curve was obtained ($y$ = 25.683 × +1.7262, $r^2$ = 1, lower limit of detection = 25 ng $mL^{-1}$).

**Plasma Stability Studies.** Fresh blood (male Balb/c mice) was collected and plasma was obtained after centrifugation (4,800 rpm by 15 min at 4 °C) as described previously.[5] Plasma diluted with isotonic sodium chloride [to 50% (v/v), 495 $\mu$L] was incubated at 37 °C for 30 min prior to the addition of the GCPQ−leucine$^5$-enkephalin formulations (5 $\mu$L, 7.23 mg $mL^{-1}$ GCPQ containing 2.78 mg $mL^{-1}$ leucine$^5$-enkephalin in 0.9% w/v sodium chloride) prepared as described above or the peptide alone (5 $\mu$L, 5 mM). The plasma was diluted to reduce the number of animals used and to slow down degradation and allow degradation to be measured. The stability of the peptide was determined in triplicate. At various time intervals, aliquots (50 $\mu$L) were removed and methanol (150 $\mu$L) was added to quench enzymatic activity. Samples were kept in −20 °C for at least 2 h prior to centrifugation (13,000 rpm for 15 min, Microcentaur, MSE, London, U.K.). The supernatant was analyzed by reverse-phase HPLC as described above for the encapsulation studies.

**Animals.** ICR (CD-1) male outbred mice (pharmacokinetic studies, 18−24 g, 4 weeks old; pharmacodynamic studies, 22−28 g, 4−5 weeks old; biodistribution/imaging studies, 20−25 g, 4−5 weeks old; Harlan, Oxon, U.K.) were housed in groups of 5 in plastic cages in controlled laboratory conditions with ambient temperature and humidity maintained at ∼22 °C and 60% with a 12 h light and dark cycle (lights on at 7:00 and off at 19:00). Food and water were available ad libitum although animals were fasted overnight for oral delivery experiments. Animals used for the tail-flick test were acclimatized in the

testing environment for at least 20 h prior to testing (lights off at 20:00 and on at 8:00, ambient temperature at 22 °C and relative humidity at 60%). All experiments were performed under license (Animals Scientific Procedures Act 1986, U.K.) and approved by the local Ethics Committee.

**Multimodal Microscopic Imaging and Sample Preparation.** Mice were administered deuterated GCPQ (75 mg $mL^{-1}$, 200 $\mu$L, 700 mg $kg^{-1}$) by oral gavage and were subsequently killed at various time points after oral dosing. Organs were harvested and stored in neutral buffered formalin (10% v/v, 15 mL). Intestine sections were tied off at either end prior to storage in formalin solution, in order to maintain the integrity of the mucous membrane. All samples for multiphoton imaging were placed between two glass coverslips using Parafilm spacers following the same procedure as Garrett et al.[8,9] Intestine and stomach samples were prepared by lateral slicing, following which the contents were removed, taking care to maintain mucous membrane integrity. Gall bladders were harvested from fixed livers and imaged whole, whereas the livers were sliced into 0.5 mm sections with razor blades in combination with a tissue slicer matrix (Zivic instruments, Pittsburgh, PA, USA).

Raman spectra were acquired using a Renishaw RM1000 Raman microscope (Renishaw, Wotton-Under-Edge, U.K.), and spectral data were acquired using Renishaw v.1.2 WiRE software. A 1200 line/mm grating giving spectral resolution of 1 $cm^{-1}$ was used with a diode laser exciting at 785 nm with up to 300 mW power. Calibration was performed using the Raman band of a silicon wafer at 520 $cm^{-1}$.

For multimodal imaging, the signal and idler excitation beams for CARS microscopy were generated using an optical parametric oscillator (OPO) (Levante Emerald, APE, Berlin, Germany) pumped by a frequency doubled Nd:vanadium picosecond oscillator (High-Q Laser Production GmbH, Hohenems, Austria), generating light at 532 nm with a 6 ps, 76 MHz pulse train. The OPO's collinear signal and idler beams have perfect temporal overlap and are continuously tunable over a range of wavelengths. The OPO signal beam (ranging from 670 to 980 nm) was used as the pump, while the idler (ranging between 1130 and 1450 nm) was used as the Stokes beam. The two beams' combined maximum output power was ~2 W, attenuation of which yielded powers at the sample of 15−30 mW. Two-photon autofluorescence (TPF) and second harmonic generation (SHG) were generated with a mode-locked femtosecond Ti:sapphire oscillator (Mira 900D; Coherent, San Jose, CA, USA) producing 100 fs pulses at 76 MHz. The central wavelength of the femtosecond beam was 800 nm, and the average power at the sample was attenuated to between 5 and 30 mW.

Imaging was performed with a modified inverted microscope and confocal laser scanner (IX71 and FV300, Olympus, Southend-on-Sea, U.K.). To optimize IR transmission, the standard galvanometer scanning mirrors and tube lens were replaced with silver galvanometric mirrors and a MgF2 coated lens respectively, while the confocal dichroic was replaced by a silver mirror (21010, Chroma Technology, Bellows Falls, VT, USA).

All multiphoton signals were collected via a 60×, 1.2 NA water immersion objective lens (UPlanS Apo, Olympus, U.K.) by directing the epi-directed signal onto an R3896 photomultiplier tube at the rear microscope port. The epi-CARS signal was separated from the pump and Stokes beams with a long-wave pass dichroic mirror (z850rdc-xr, Chroma Technologies Corp.). The anti-Stokes signal was isolated with a single band-pass filter centered at 750 nm (HQ750/210, Chroma Technologies Corp.). TPF and SHG signal was first spectrally separated from the 800 nm excitation beam with a dichroic mirror (670dcxr; Chroma Technologies). Different bandpass filters were employed to direct either the TPF signal (CG-BG-39-1.00-1 and F70-500-3-PFU; CVI Melles Griot, Cambridge, U.K.) or SHG signal (F10-400-5-QBL; CVI Melles Griot, U.K.) to the photomultiplier tube.

**Biodistribution of Radiolabeled GCPQ.** Mice were dosed by oral gavage with purified $^{125}$I-GCPQ [200 $\mu$L (1−1.3 × $10^6$ counts), 200 mg $kg^{-1}$]. At various time points, animals were killed, blood and organs harvested and radioactivity levels immediately counted (Perkin-Elmer Wallac Wizard II automatic gamma counter, Perkin-Elmer, Cambridge, U.K.).

**Pharmacokinetics of GCPQ−Leucine$^5$-enkephalin Nanoparticles.** Mice were administered by oral gavage either water or various leucine$^5$-enkephalin (70 mg $kg^{-1}$) formulations. The dose volume varied by animal weight but was less than 150 $\mu$L per mouse. Animals were killed at various time points and the blood, brain and liver sampled. Liver samples (0.5−0.8 g) were homogenized and extracted in an identical manner to brain samples.[5] Leucine$^5$-enkephalin levels were analyzed in blood, brain and liver samples using a radioimmunoassay kit as previously described.[5]

**Pharmacodynamics: The Tail-Flick Bioassay.** Antinociception was assessed in mice using the tail flick warm water bioassay[11,12] as described previously.[5] Mice not responding within 5 s were excluded from further testing, and the baseline latency was measured for all mice 2 h prior to testing. Maximum possible exposure time to the thermal stimuli was set at 10 s to avoid unnecessary damage to the tail.[13] A maximum score was assigned (100%) to animals not responding to the thermal stimuli (with a sharp tail flick) within 10 s. The response times were then converted to percentage of maximum possible effect (% MPE) by a method reported previously.[14] Data are also presented in the quantal form of the tail flick test (number of mice that exhibited maximum latencies to thermal stimuli − the maximum possible effect) which ensures no false positive responses.[11] An analgesic responder was defined as one whose tail flick latency was two or more times the value of the baseline latency.[15]

**Statistics.** Statistical analyses were performed using either Student's $t$ test or one-way ANOVA along with post hoc analysis using Tukey's test (95% CI) and performed with Minitab 15 software (Coventry, U.K.).

## RESULTS

**Polymer Synthesis.** Four amphiphilic polymers of different molecular weights were synthesized in good yield and characterized; molecular weights ranged from 6 to 58 kDa (Table 1). Various deuterated amphiphiles were also obtained in good yield (Table 1). Acid degradation of glycol chitosan reduces the polymer molecular weight in a nonlinear manner[10] (Table SI-1 in the Supporting Information). The depolymerization reaction is a first order reaction[10] making it difficult to yield the lowest molecular weight polymers. The first order rate constant is −1.346 ($M_n$ = 94448 $e^{-1.346t}$ + 7041, $r^2$ = 0.99901). We used a new re-degradation strategy to obtain GC6 from GC10 and were able to generate a 4 kDa polymer with low polydispersity (Table SI-1 in the Supporting Information). The only alternative strategy to the production of such low molecular weight chitosans (<10 kDa) is the use of nitrous

acids, but polymers resulting from nitrous acid degradation possess terminal aldehyde groups;[16] such aldehyde groups may cross-link biological proteins on administration in vivo. A further concern would be the potential long-term toxicity of such polymers due to the production of carcinogenic nitrosamines.[17]

**GCPQ Nanoparticles.** GCPQ amphiphiles give rise to stable (CMCs in the $\mu$M range),[6,7] nanosized aggregates (Figure 1). With the exception of GCPQ50 all polymers present as low viscosity dispersions (Table 1). Particle size increases with molecular weight with GCPQ6 particles being 80 nm in size, GCPQ 10 particles being 110 nm in size and GCPQ50 particles being 600 nm in size (Figure 1). We have previously shown that the size of polymeric particles is directly governed by the molecular weight of the self-assembling polymers.[10]

**Leucine$^5$-enkephalin Antinociceptive Activity.** Previously we have shown that GCPQ particles formed from 14 kDa GCPQ (GCPQ14) delivered leucine$^5$-enkephalin through the oral route to the brain, increasing brain exposure by 67%.[5] In order to uncover the mechanism of action, we have assessed the effect of GCPQ–leucine$^5$-enkephalin particles (prepared from GCPQs of different molecular weight) on antinociceptive activity after oral administration. Only the GCPQ50 and GCPQ10 formulations produce significant antinociceptive activity, with antinociception lasting over 6–8 h (Figure 2). Furthermore, only the GCPQ50 and GCPQ10 formulations are able to produce the maximum possible pharmacological effect (Table 2). GCPQ14 also produces maximum possible effect responders.[5] By contrast, the peptide alone and the GCPQ6 formulation are therapeutically inactive via the oral route (Figure 2). We conclude that a GCPQ molecular weight in excess of 6 kDa is required to achieve a pharmacological response.

**Leucine$^5$-enkephalin Pharmacokinetics.** The oral administration of the GCPQ6 and GCPQ50 leucine$^5$-enkephalin formulations increased plasma exposure to leucine$^5$-enkephalin, when compared to the drug alone (Figure 3a, Table 2). However while the GCPQ6 formulation produced slightly more brain exposure at the early half-hour time point (Figure 3b), this was not sustained, in contrast to the GCPQ50 formulation, which increased brain exposure at the 1 and 2 h time points, leading to a sustained and significantly increased brain exposure compared to leucine$^5$-enkephalin peptide alone (Figure 3b, Table 2). In order to arrive at an estimation of the brain parenchyma drug levels, we took into account the brain plasma volume[18−20] and the plasma drug levels and found that brain parenchyma levels account for at least 98% of the brain levels quoted in Table 2 (Table SI-2 in the Supporting Information). We have previously reported that brain exposure to leucine$^5$-enkephalin was increased by 67% by GCPQ14 and that this exposure differential was sustained.[5] We conclude that while a range of GCPQ nanoparticle formulations are able to improve plasma levels of leucine$^5$-enkephalin via the oral route, only those nanoparticles prepared from polymers with a molecular weight in excess of 6 kDa are capable of improving brain exposure after oral administration.

Liver $AUC_{0-24}$ levels were lower than seen in the brain (Figure 3c, Table 2), presumably as a result of active degradation of leucine$^5$-enkephalin in the liver. GCPQ nanoparticles did not protect the peptide from degradation in the liver.

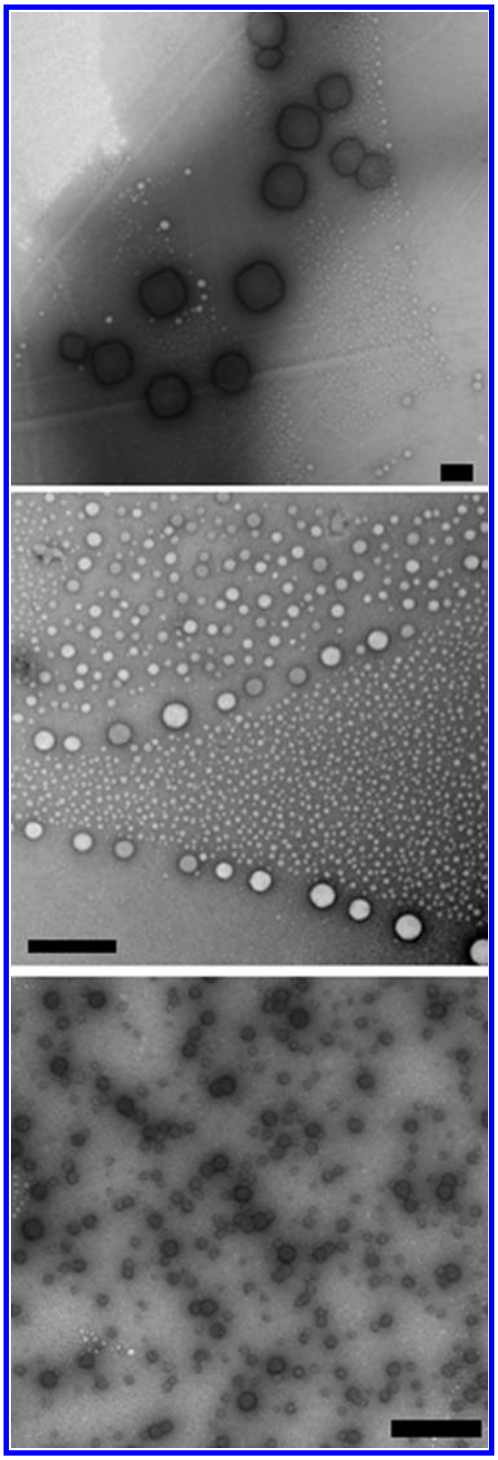

**Figure 1.** Transmission electron microscopy (TEM) images of freshly prepared: (a) GCPQ50 (75 mg mL$^{-1}$)–leucine$^5$-enkephalin (15 mg mL$^{-1}$) nanoparticles, (b) GCPQ10 (75 mg mL$^{-1}$)–leucine$^5$-enkephalin (15 mg mL$^{-1}$) nanoparticles, (c) GCPQ6 (75 mg mL$^{-1}$)–leucine$^5$-enkephalin (15 mg mL$^{-1}$) nanoparticles, bars = 500 nm.

**Leucine$^5$-enkephalin Plasma Stability.** GCPQ50 in a similar manner to GCPQ14[5] protects leucine$^5$-enkephalin from plasma degradation in vitro (Figure 4), increasing the in vitro plasma half-life slightly from 18 to 20 min. In contrast, GCPQ6 does not protect leucine$^5$-enkephalin from plasma degradation in vitro (Figure 4). GCPQ14 protects leucine$^5$-enkephalin from

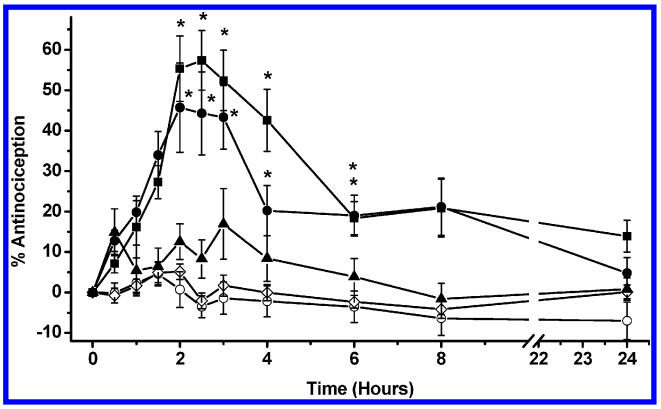


**Figure 2.** Central analgesic effects as demonstrated using the tail flick bioassay after the oral administration of leucine$^5$-enkephalin (70 mg kg$^{-1}$) formulations to mice: water (○), leucine$^5$-enkephalin (◇), GCPQ6–leucine$^5$-enkephalin (polymer weight ratio = 5:1) (▲), GCPQ10–leucine$^5$-enkephalin (polymer weight ratio = 5:1) (●), GCPQ50–leucine$^5$-enkephalin (polymer weight ratio = 5:1) (■) (mean ± SEM, $n \geq 10$), * = significantly different when compared to leucine$^5$-enkephalin ($p < 0.05$) .

**Table 2. Pharmacokinetics and Pharmacodynamics Data on GCPQ–leucine$^5$-enkephalin Formulations**

| | AUC$_{0-24}$ (ng mL$^{-1}$ h) | | | | |
|---|---|---|---|---|---|
| formulation | plasma | brain | liver | % responders | % responders showing max possible effect |
| leucine$^5$-enkephalin | 1454 | 1842 | 202 | 0 | 0 |
| GCPQ6–leucine$^5$-enkephalin | 2357[a] | 2060 | 222 | 30 | 0 |
| GCPQ50–leucine$^5$-enkephalin | 2358[a] | 2081[a] | 175 | 90 | 10 |

[a]Statistical significance compared to leucine$^5$-enkephalin alone, $p < 0.05$.

plasma degradation in vitro and increases the drug's plasma half-life by 91% in vitro.[5] We conclude that a minimal GCPQ molecular weight (>6 kDa) is required to enable the protection of peptides from degradation in plasma. This protection from plasma degradation is important as leucine$^5$-enkephalin has a short plasma half-life of ($t_{1/2}$ = 3 min[21]); even a modest protection from degradation would prolong plasma residence time and have a positive effect on drug pharmacokinetics/pharmacodynamics.

In order to further understand how polymer molecular weight affects drug degradation in plasma, we examined the effect of molecular weight on peptide encapsulation as better encapsulation would be expected to reduce degradation. We found that the encapsulation of leucine$^5$-enkephalin in GCPQ nanoparticles is indeed molecular weight dependent with GCPQ50 encapsulating double the amount of the hydrophilic peptide compared to the polymers with molecular weight ≤14 kDa (Figure 5). This encapsulation and protection in plasma could potentially explain the increase in the brain exposure to leucine$^5$-enkephalin with GCPQ50 nanoparticles compared to GCPQ6 nanoparticles.

**GCPQ Pharmacokinetics.** In an effort to understand the role of particle absorption on oral brain delivery, we investigated the oral biodistribution of radiolabeled GCPQ

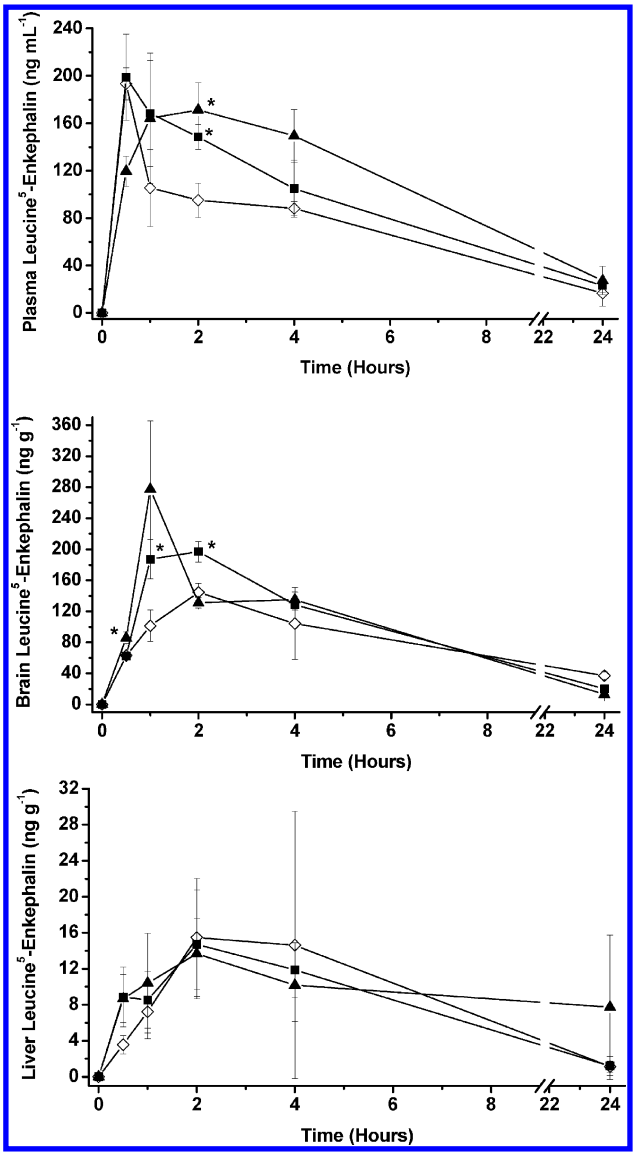


**Figure 3.** Leucine$^5$-enkephalin levels in plasma, brain and liver after the oral administration of leucine$^5$-enkephalin (70 mg kg$^{-1}$) to mice: leucine$^5$-enkephalin (◇), GCPQ6–leucine$^5$-enkephalin (polymer weight ratio = 5:1) (▲), GCPQ50–leucine$^5$-enkephalin (polymer weight ratio = 5:1) (■) (mean ± sem, $n$ = 5), * = significantly different when compared to leucine$^5$-enkephalin ($p < 0.05$).

particles (Figure 6). This is the first study to quantify the fate of chitosan amphiphile nanoparticles after oral administration. First of all it is important to state that total recovery of in vivo radioactivity for all time points was very high at 90%, with the exception of the 24 h time point, for which more than 60% of radioactivity was recovered. Importantly, the iodine label remained intact as the level of activity found in the thyroid was minimal with only 0.1% of the dose being found at the early time points (under 4 h) (Figure 6m). Thyroid levels are a surrogate marker for radiolabel stability and an indication of the level of free iodine administered or generated in vivo. For GCPQ14, the polymer with the highest level of particle absorption (Figure 6a), thyroid levels remained low throughout all time points studied (Figure 6m).

While the majority of the GCPQ nanoparticle dose (85–90% of the administered dose) remains in the gastrointestinal tract up to 1 h after dosing (Figure 6), a fraction of the nanoparticle


dx.doi.org/10.1021/mp300068j | Mol. Pharmaceutics 2012, 9, 1764–1774

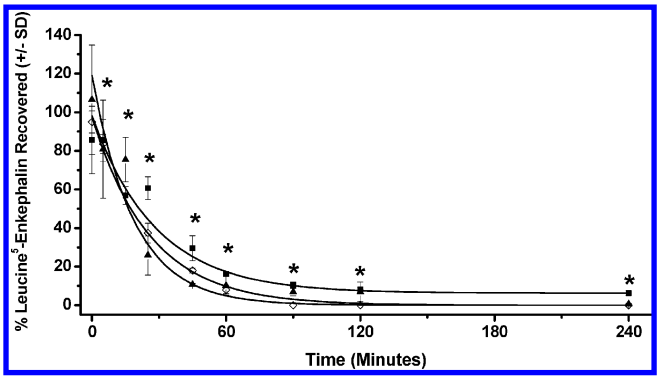


**Figure 4.** In vitro peptide stability. The stability of various peptide formulations (final concentration of leucine$^5$-enkephalin = 2.78 mg mL$^{-1}$) in plasma (50% v/v): leucine$^5$-enkephalin (◇), GCPQ6–leucine$^5$-enkephalin (polymer, weight ratio = 2.6:1) (▲), GCPQ50–leucine$^5$-enkephalin (polymer, weight ratio = 2.6:1) (■) (mean ± SD, $n$ = 3), * = significantly different when compared to leucine$^5$-enkephalin ($p < 0.05$).

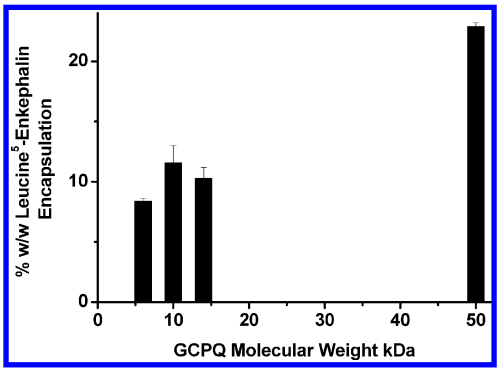


**Figure 5.** Encapsulation of leucine$^5$-enkephalin in various GCPQ formulations.

dose was absorbed and found in the blood and liver (1–6% of the administered dose, Figures 6a and 6b), with GCPQ14 absorption being superior to the absorption of GCPQ6 and GCPQ50. The oral bioavailability of GCPQ14 is calculated to be 23.7%; this figure is calculated from the plasma $AUC_{0-24}$ after oral (Figure 6a) and intravenous[5] administration of radiolabeled GCPQ. This is the first report of the oral bioavailability for chitosan nanoparticles. A peak plasma concentration of 3% of the dose does at first seem at odds with the absolute bioavailability data, but the absolute bioavailability is effectively a proportion of the intravenous drug exposure and not a proportion of the dose. For example oral ranitidine (Zantac) has a peak plasma level of 2.5% of the dose in rats,[6] a peak plasma level of 0.5% of the dose in humans[22] and a bioavailability of 56% in humans.[22] Only minor amounts of radiolabeled GCPQ (<0.5% of the administered dose) were found in other major organs outside the gastrointestinal tract (Figure 6). However in the kidneys/urethra (Figure 6h) and the skin (Figure 6p) 1–2% of the administered dose was found. On intravenous administration, GCPQ is excreted via the kidneys/urethra,[5] and it is conceivable that excretion of orally absorbed GCPQ also takes place via the kidneys. We are unsure why higher levels were seen in the skin when compared to other organs, although we speculate that the skin levels may be a reflection of particles adhering to blood capillaries. As well as being excreted through the kidneys, the polymer remaining in the gastrointestinal tract was excreted within the feces (Figure 6j). When administered orally, GCPQ particles are not found in the brain (Figure 6l). The level of radiolabeled GCPQ in the carcass reflects levels in the bone and muscle mass (Figure 6o), and there is significantly less radiolabeled GCPQ14 in the bone and muscle mass, when compared to GCPQ6 and GCPQ50 nanoparticles.

An interesting observation confirming the absorption of GCPQs was the rise in the radiolabeled GCPQ signal seen in the gall bladder two hours after oral administration (Figure 6c), indicative of particles accumulating in the bile from the liver (Figure 6b).

**Multimodal ex Vivo Imaging.** In order to determine whether the radioactivity observed in various tissues was due to the presence of nanoparticles in these tissues, we utilized a combination of CARS, second harmonic generation and two photon fluorescence microscopy to selectively image particles pinpointed with subcellular precision[8,9]within the gastrointestinal tract, the liver and the gall bladder (Figure 7). Using particles prepared from deuterated GCPQ, chemically identical to the GCPQ used in the quantitative radiolabel studies, we were able to ascertain that the polymer was present in the form of particles in these tissues.

CARS microscopy of liver, stomach, duodenum, jejunum, ileum and gall bladder after oral dosing of deuterated GCPQ shows deuterated particles present in these tissues (Figure 7), supporting our interpretation that GCPQ particles are absorbed and adding further support to our hypothesis on particle absorption being fundamental to peptide absorption. Deuterated particles of 50 kDa GCPQ appear to be located in the intercellular spaces between hepatocytes (which correlates well with the location of liver sinusoids and bile canaliculi) (Figure 7 a), the smooth muscle cells of the stomach (Figure 7b), the collagen network of the jejunum (Figure 7c) within the villi (having crossed the enterocytes into the villi) of the ileum and duodenum (Figures 7d and 7e) and within the gall bladder (Figure 7f). We have previously shown that GCPQ particles are present within hepatocytes and at the boundary of the submucosa and the muscularis propria below the base of the villi,[9] and although others have shown that particle uptake in the gut is a principal function of the Peyer's patches,[23] we have examined Peyer's patches after dosing with Texas Red labeled GCPQ and found no evidence of GCPQ uptake (data not shown).

## ■ DISCUSSION

The oral use of neuropeptides to treat brain disorders is not currently possible due to a combination of factors: (a) peptide degradation from soluble and brush border enzymes in the gut, (b) the presence of the gastrointestinal mucus layer (100–150 μm) hindering the access of peptides to the absorptive enterocytes, (c) ultimately limited oral peptide absorption due to poor permeability and lack of active transport mechanisms, (d) degradation of peptides in the plasma and (e) poor peptide permeability and the lack of uptake mechanisms at the BBB. Leucine$^5$-enkephalin is a small endogenous opioid pentapeptide with a short serum half-life of 3 min in humans.[21] Leucine$^5$-enkephalin is hydrolyzed in the gut primarily by brush border metalloproteases such as aminopeptidases and particularly by aminopeptidase N as well as by trypsin followed by dipeptidylaminopeptidases and dipeptidylcarboxypeptidases.[24,25]

While GCPQ nanoparticles promote the oral absorption and brain delivery of neuropeptides such as leucine$^5$-enkephalin,[5]

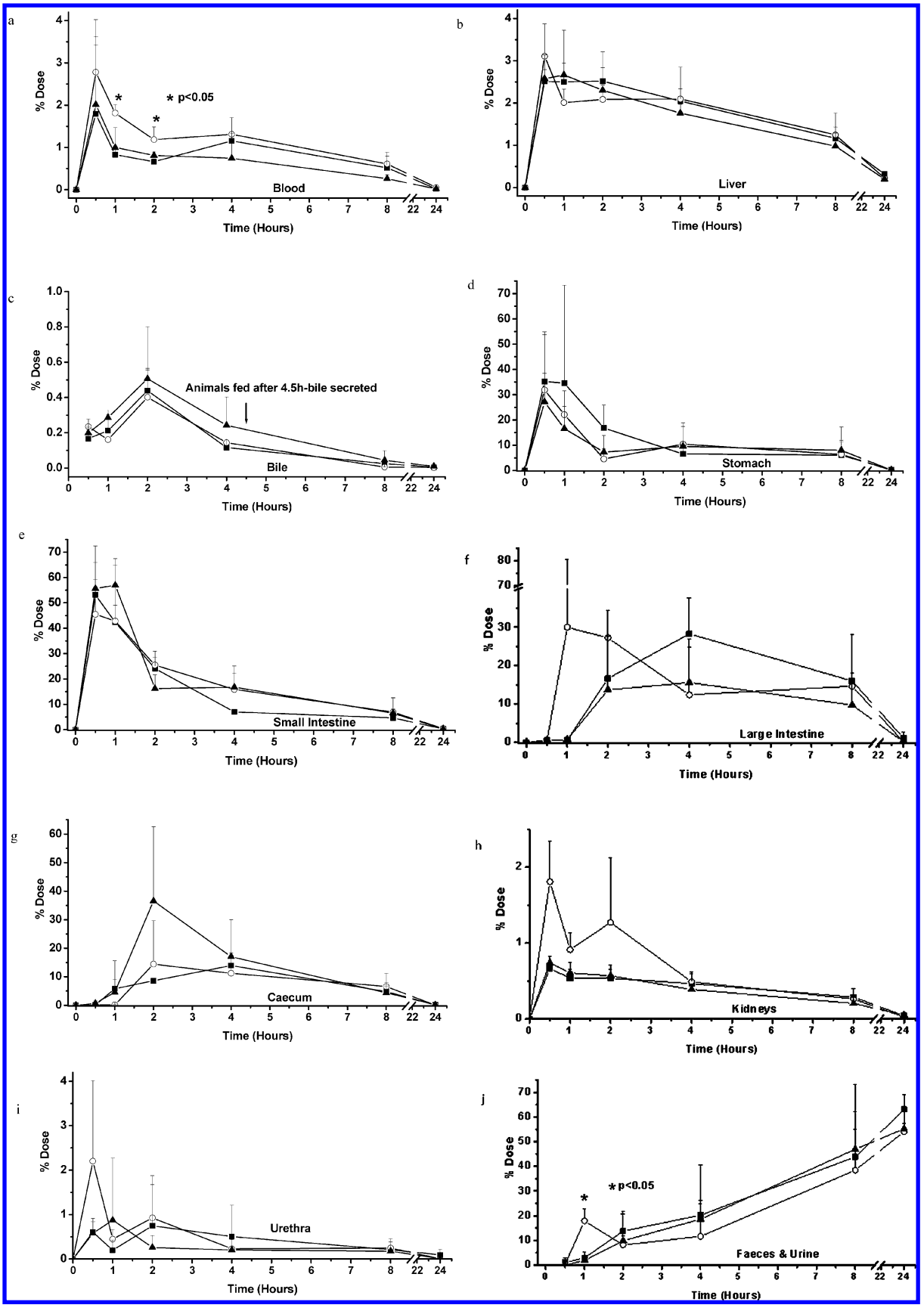


**Figure 6.** continued


dx.doi.org/10.1021/mp300068j | *Mol. Pharmaceutics* 2012, 9, 1764−1774

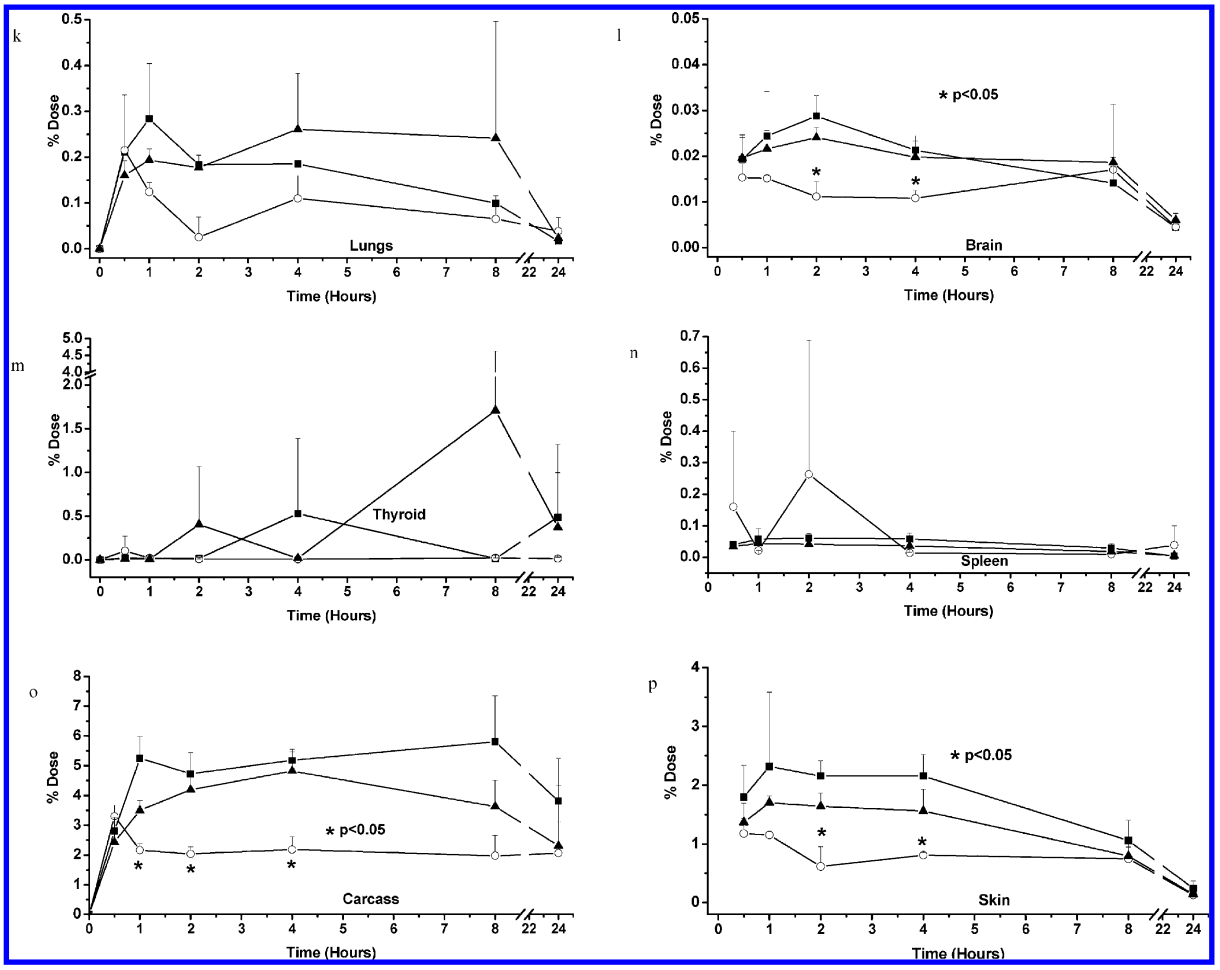


**Figure 6.** % of radioactivity dose recovered from various organs following the oral administration of $^{125}$I-GCPQ nanoparticles (200 mg kg$^{-1}$): ■ = GCPQ50, ○ = GCPQ14, ▲ = GCPQ6 (mean ± SD, $n$ = 3), * = significantly different when compared to $^{125}$I-GCPQ6 and $^{125}$I-GCPQ50 ($p < 0.05$).

the mechanism by which GCPQ nanoparticles deliver peptides orally to the brain is unclear. Here we establish key facts about the mechanism of action of GCPQ particles, which could also serve as a blueprint for other nanoparticles.

In previous studies we have established that GCPQ nanoparticles protect peptides such as leucine$^5$-enkephalin from intestinal enzymatic degradation.[5] Furthermore we have demonstrated the ability of GCPQ particles to penetrate through the mucus layer to promote intimate contact with the enterocytes.[6] Here we report for the first time that polymeric chitosan nanoparticles are detected within the villi, following oral dosing (Figure 7c and 7d), presumably absorbed via the enterocytes. We know that 11−23% of the peptide is associated with the particles (Figure 5) and also that more peptide is found in the plasma with GCPQ nanoparticle formulations when compared to the administration of the peptide alone (Figure 3a), indicating that peptide oral absorption is correlated with particle uptake. GCPQ does not open epithelial tight junctions[6] thus precluding the possibility of paracellular peptide transport. Our data further suggests that once within the plasma the peptide is stabilized from degradation by GCPQ (Figure 4), and while the in vitro plasma half-life of the peptide is only increased by 10% by association with GCPQ50 nanoparticles, this is sufficient to improve the brain levels of the peptide (Figure 3b) and elicit antinociceptive activity (Figure 2). The peptide is presumed to cross the BBB, when the GCPQ particles make contact with the brain endothelial cells. We know that intravenously administered polymer particles circulate in the bloodstream and adhere to the perivascular spaces of arterioles and venules and the inner surface of blood vessel endothelial cells in the brain,[8] enabling the peptide to cross the blood−brain barrier .

Increased plasma stability of leucine$^5$-enkephalin when administered orally in GCPQ nanoparticles is further supported by the statistically significant increase in plasma $AUC_{0-24}$ for the peptide when encapsulated within GCPQ nanoparticles (Table 2). Indirect evidence that GCPQ−leucine$^5$-enkephalin particle absorption is important for peptide activity may be found in the difference in brain exposure (Figure 3b) and pharmacodynamic activity (Figure 2) when the GCPQ6 and GCPQ50 formulations are compared. The differing brain exposure/pharmacodynamic activity associated with similar levels of plasma exposure (Figure 3a) demonstrates that the leucine$^5$-enkephalin present in the plasma is not identical in format across the two polymer formulations: GCPQ50 and GCPQ6. We hypothesize that the greater brain exposure found with GCPQ50 formulations is due to the fact that the GCPQ50−leucine$^5$-enkephalin formulation stabilizes leucine$^5$-enkephalin within the plasma to a greater extent than the GCPQ6−leucine$^5$-enkephalin formulation (Figure 4), possibly because GCPQ50 nanoparticles are more avid encapsulators of leucine$^5$-enkephalin (Figure 5). One aspect which needs discussing is the fact that plasma levels of leucine$^5$-enkephalin with GCPQ50 formulations are not superior to those obtained

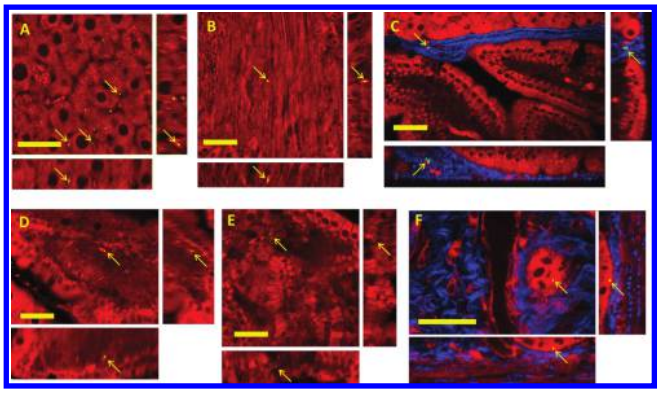


**Figure 7.** Orthogonal views of reconstructed three-dimensional multiphoton image stacks taken of mouse samples harvested 60 min after oral dosing with GCPQ50 particles (600 mg $kg^{-1}$). (a) Liver tissue imaged with epi-CARS with contrast derived from the $CD_2$ and $CH_2$ resonances using $\omega p - \omega s$ tuned to 2100 $cm^{-1}$ (green) and 2845 $cm^{-1}$ (red) respectively; GCPQ50 particles are seen within the hepatocellular spaces. (b) Stomach tissue samples imaged with epi-CARS with contrast derived from the $CD_2$ and $CH_2$ resonances using $\omega p - \omega s$ tuned to 2100 $cm^{-1}$ (green) and 2845 $cm^{-1}$ (red) respectively; particles are seen associated with the smooth muscle cells lining the stomach wall. (c) Jejunum tissue imaged with epi-CARS with contrast derived from the $CD_2$ resonance (green), SHG contrast derived from collagen (blue) and TPF contrast derived from endogenous fluorophores (red); particles are seen associating with the collagen tissue found between the base of the villi/intestinal crypts and the muscularis mucosae. (d) Ileum tissue imaged with epi-CARS with contrast derived from the $CD_2$ and TPF (red); particles are seen within the villi having crossed the enterocytes. (e) Duodenum imaged with epi-CARS with contrast derived from the $CD_2$ and TPF (red); particles are seen within the villi having crossed the enterocytes. (f) Gall bladder imaged with epi-CARS with contrast derived from the $CD_2$ resonance (green), SHG (blue) and TPF (red); particles are seen associating with the cells lining the mucosal folds. All scale bars are 40 $\mu$m. Arrows indicate the position of particle signal.

with GCPQ6 formulations, and we can only conclude that the leucine[5]-enkephalin measured in the blood takes into account particle bound and non particle bound material and that the brain transport of particle bound material is favored over that of non particle bound material, for the reasons given above.

The increase in radiolabeled GCPQ signal observed in the gall bladder, reaching a maximum level two hours following oral administration (Figure 6c), is indicative of particles accumulating in the bile from the liver after absorption into the blood and distribution to the liver (Figure 6b). We know that GCPQ polymers are absorbed from the GCPQ biodistribution data (Figure 6) and that GCPQ nanoparticles are absorbed from CARS imaging data (Figure 7).

The plasma $T_{max}$ indicates that absorption takes place in the upper gastrointestinal tract. Although chitosan polymer absorption has been reported previously utilizing FITC-labeled chitosans,[26,27] this is the first report of the absorption of chitosan nanoparticles (Figure 7). The CARS imaging data show that GCPQ particles are circulated from the villi to the liver, to the gall bladder and presumably back to the gastrointestinal tract.

Chitosans with molecular weights between 5 and 50 kDa have been shown to bind lipids and bile salts[28] with 1 g of chitosan able to bind 2−3 g of bile salts such as cholic acid and sodium taurocholate.[29,30] The binding of GCPQ particles with bile salts is thus a distinct possibility. To arrive in the gall bladder from the liver and ultimately from the blood, radiolabeled GCPQ (possibly bound to bile salts), once having traversed the villi epithelium, would be able to enter the blood via either the villi's lymphatic vessels or the villi's blood vessels. The gut's lymphatic vessels are able to carry particulate entities such as chylomicrons and lipoprotein particles. These vessels link to the mesenteric lymphatic network, and ultimately, via the thoracic duct, the systemic blood circulation. This is the route the lipid loaded chylomicrons and lipoproteins take to reach the liver for metabolic processing.[31] Alternatively venous blood from the ileum containing the particles could be transported to the liver via the portal vein.

Once radiolabeled GCPQ arrives at the liver, hepatocytes would extract the bile acids from sinusoidal blood and transport the bile acids and associated polymer across the hepatocytes to be resecreted into canaliculi. We assert, in effect, that the radiolabeled GCPQ circulates from the villi to the liver to the gall bladder and will arrive back in the intestine once the bile is released (Figures 6a−c).

We thus conclude that GCPQ particles are absorbed via the enterocytes and transported to the liver via the gut lymphatic vessels or venous blood in the villi; from the liver, particles are transported on to the gall bladder where they are most likely then circulated back to the gastrointestinal tract. The quantitative (Figure 6) and imaging (Figure 7) evidence all support the oral absorption and enterohepatic circulation of GCPQ nanoparticles.

Now that we have established that particle absorption is crucial for oral peptide delivery, we have a number of ways in which GCPQ formulations may be optimized. Drug association with the particles could be increased and an optimum polymer molecular weight used. It is interesting to note that GCPQ14 nanoparticles, orally absorbed to a greater extent than both GCPQ50 and GCPQ6 nanoparticles (Figure 6a), increase brain exposure by 67% and produce 38% maximum possible effect responders,[5] whereas GCPQ50 increases brain exposure by 10% and produces 10% maximum possible effect responders.

## ■ CONCLUSIONS

We have established a mechanism for polymer-enabled oral to brain delivery of a gut-labile and plasma-labile peptide. GCPQ nanoparticle peptide formulations adhere to the gastrointestinal mucosa bringing the particles in close contact with the absorptive enterocytes. GCPQ particles cross the enterocytes and are transported to the blood, on to the liver and onward to the gall bladder, effectively circulating. Once in the blood the particles stabilize the peptide from degradation and polymer associated peptide adheres to the plasma surface of the brain endothelial cells, enabling the peptide to cross the blood−brain barrier. We have no evidence of GCPQ crossing the BBB after oral administration, and GCPQ does not appreciably cross the BBB[5] following intravenous administration; the CARS signal for GCPQ is only seen occasionally within the brain parenchyma[8] following intravenous administration. The activity of GCPQ is molecular weight dependent, and a molecular weight in excess of 6 kDa is required for brain pharmacodynamic activity.

## ■ ASSOCIATED CONTENT

### Supporting Information

Tables summarizing the characterization of glycol chitosan (GC) polymer samples and the brain parenchyma levels. This

material is available free of charge via the Internet at http://pubs.acs.org.

## AUTHOR INFORMATION


### Corresponding Author

*UCL School of Pharmacy, University of London, 29-39 Brunswick Square, London, WC1N 1AX, U.K. E-mail: ijeoma.uchegbu@ucl.ac.uk. Tel: +44 (0) 207 753 5997. Fax: +44 (0) 207 753 5942.

### Present Address

[§]Department of Pharmaceutical Sciences, University of Calabria, 87036 Arcavacata di Rende, Cosenza, Italy.


### Notes

The authors declare no competing financial interest.

## ACKNOWLEDGMENTS

Financial support from the Engineering and Physical Sciences Research Council (EPSRC) and GlaxoSmithKline (GSK). David McCarthy (UCL School of Pharmacy) is acknowledged for providing transmission electron microscopy expertise.

## REFERENCES


(1) Tauzin, B. *Biotechnology Medicines in Development*; Pharmaceutical Research and Manufacturers Association: Washington, DC, 2006.

(2) Karls, M. S.; Rush, B. D.; Wilkinson, K. F.; Vidmar, T. J.; Burton, P. S.; Ruwart, M. J. Desolvation Energy—a Major Determinant of Absorption, but Not Clearance, of Peptides in Rats. *Pharm. Res.* **1991**, *8* (12), 1477−81.

(3) Pauletti, G. M.; Gangwar, S.; Siahaan, T. J.; Aube, J.; Borchardt, R. T. Improvement of oral peptide bioavailability: Peptidomimetics and prodrug strategies. *Adv. Drug Delivery Rev.* **1997**, *27* (2−3), 235−56.

(4) Lalatsa, A.; Schätzlein, A. G.; Uchegbu, I. F. Drug delivery across the blood brain barrier. In *Comprehensive Biotechnology*, 2nd ed.; Murray Moo-Young, M., Butler, M., Webb, C., Moreira, A., Grodzinski, B., Cui, Z., Eds.; Elsevier: Amsterdam, 2011; pp 657−68.

(5) Lalatsa, A.; Lee, V. L.; Schätzlein, A. G.; Malkinson, J.; Uchegbu, I. F. A prodrug nanoparticle approach for the delivery of peptides to the brain via the oral and intravenous routes. *Mol. Pharmaceutics* **2012**, DOI: dx.doi.org/10.1021/mp300009u.

(6) Siew, A.; Thiovolet, M.; Sinis, F.; Gellert, P.; Schätzlein, A. G.; Uchegbu, I. F. Enhanced Oral Absorption of Hydrophobic and Hydrophilic Drugs Using Quaternary Ammonium Palmitoyl Glycol Chitosan Nanoparticles. *Mol. Pharmaceutics* **2012**, *9* (1), 14−28.

(7) Qu, X.; Khutoryanskiy, V. V.; Stewart, A.; Rahman, S.; Papahadjopoulos-Sternberg, B.; Dufes, C.; McCarthy, D.; Wilson, C. G.; Lyons, R.; Carter, K. C.; Schätzlein, A.; Uchegbu, I. F. Carbohydrate-based micelle clusters which enhance hydrophobic drug bioavailability by up to 1 order of magnitude. *Biomacromolecules* **2006**, *7* (12), 3452−9.

(8) Garrett, N.; Lalatsa, A.; Begley, D.; Mihoreanu, L.; Schätzlein, A.; Uchegbu, I.; Moger, J. Label-free imaging of polymeric nanomedicines using coherent anti-Stokes Raman scattering microscopy. *J. Raman Spectrosc.* **2012**, DOI: 10.1002/jrs.3170.

(9) Garrett, N.; Lalatsa, A.; Schätzlein, A.; Uchegbu, I.; Moger, J. Distribution of polymeric nanoparticles in the gut and liver, imaged using multiphoton microscopy. *J. Biophotonics* **2012**, *5*, 458−468.

(10) Wang, W.; McConaghy, A. M.; Tetley, L.; Uchegbu, I. F. Controls on polymer molecular weight may be used to control the size of palmitoyl glycol chitosan polymeric vesicles. *Langmuir* **2001**, *17*, 631−6.

(11) D'Amour, F. E.; Smith, D. L. A method for determining loss of pain sensation. *J. Pharmacol. Exp. Ther.* **1941**, *72*, 74−9.

(12) Mogil, J. S.; Wilson, S. G.; Bon, K.; Lee, S. E.; Chung, K.; Raber, P.; Pieper, J. O.; Hain, H. S.; Belknap, J. K.; Hubert, L.; Elmer, G. I.; Chung, J. M.; Devor, M. Heritability of nociception I: responses of 11 inbred mouse strains on 12 measures of nociception. *Pain* **1999**, *80* (1−2), 67−82.

(13) Tjolsen, A.; Hole, K. The tail-flick latency is influenced by skin temperature. *AAPS J.* **1993**, *2*, 107−11.

(14) Polt, R.; Porreca, F.; Szabo, L. Z.; Bilsky, E. J.; Davis, P.; Abbruscato, T. J.; Davis, T. P.; Harvath, R.; Yamamura, H. I.; Hruby, V. J. Glycopeptide enkephalin analogues produce analgesia in mice: evidence for penetration of the blood-brain barrier. *Proc. Natl. Acad. Sci. U.S.A.* **1994**, *91* (15), 7114−8.

(15) Shimoyama, N.; Shimoyama, M.; Elliott, K. J.; Inturrisi, C. E. d-Methadone is antinociceptive in the rat formalin test. *J. Pharmacol. Exp. Ther.* **1997**, *283* (2), 648−52.

(16) Tommeraas, K.; Varum, K. M.; Christensen, B. E.; Smidsrod, O. Preparation and characterisation of oligosaccharides produced by nitrous acid depolymerisation of chitosans. *Carbohydr. Res.* **2001**, *333* (2), 137−44.

(17) Knight, D. K.; Shapka, S. N.; Amsden, B. G. Structure, depolymerization, and cytocompatibility evaluation of glycol chitosan. *J. Biomed. Mater. Res., Part A* **2007**, *83* (3), 787−98.

(18) Rapoport, S. I.; Fitzhugh, R.; Pettigrew, K. D.; Sundaram, U.; Ohno, K. Drug entry into and distribution within brain and cerebrospinal fluid: [14C]urea pharmacokinetics. *Am. J. Physiol.* **1982**, *242* (3), R339−48.

(19) Smith, Q. R.; Allen, D. D. In Situ Brain Perfusion Technique. In *Methods in Molecular Medicine, The Blood−Brain Barrier: Biology and Research Protocols*; Nag, S., Ed.; Humana Press Inc.: Totowa, 2003; Vol. *89*, pp 209−18.

(20) Takasato, Y.; Rapoport, S. I.; R., S. Q. An in situ brain perfusion technique to study cerebrovascular transport in the rat. *Am. J. Physiol.* **1984**, *247*, H484−93.

(21) Hussain, M. A.; Rowe, S. M.; Shenvi, A. B.; Aungst, B. J. Inhibition of leucine enkephalin metabolism in rat blood, plasma and tissues in vitro by an aminoboronic acid derivative. *Drug. Metab. Dispos.* **1990**, *18* (3), 288−91.

(22) Garg, D. C.; Weidler, D. J.; Eshelman, F. N. Ranitidine bioavailability and kinetics in normal male subjects. *Clin. Pharmacol. Ther.* **1983**, *33* (4), 445−52.

(23) Hussain, N.; Jaitley, V.; Florence, A. T. Recent advances in the understanding of uptake of microparticulates across the gastrointestinal lymphatics. *Adv. Drug Delivery Rev.* **2001**, *50* (1−2), 107−42.

(24) Bernkop-Schnurch, A.; Paikl, C.; Valenta, C. Novel bioadhesive chitosan-EDTA conjugate protects leucine enkephalin from degradation by aminopeptidase N. *Pharm. Res.* **1997**, *14* (7), 917−22.

(25) Woodley, J. F. Enzymatic barriers for GI peptide and protein delivery. *Crit. Rev. Ther. Drug Carrier Syst.* **1994**, *11* (2−3), 61−95.

(26) Chae, S. Y.; Jang, M. K.; Nah, J. W. Influence of molecular weight on oral absorption of water soluble chitosans. *J. Controlled Release* **2005**, *102* (2), 383−94.

(27) Zeng, L.; Qin, C.; Wang, W.; Chi, W.; Li, W. Absorption and distribution of chitosan in mice after oral administration. *Carbohydr. Polym.* **2008**, *71*, 435−440.

(28) Sugano, M.; Watanabe, S.; Kishi, A.; Izume, M.; Ohtakara, A. Hypocholesterolemic action of chitosans with different viscosity in rats. *Lipids* **1988**, *23* (3), 187−91.

(29) Meler, J.; Pluta, J. 10. Investigation of bile acid salts binding capacity by various kinds of chitosans. In *Polish Chitin Society, Monograph XI*; **2006**; pp 79−83.

(30) Thongngam, M.; McClements, D. J. Characterization of interactions between chitosan and an anionic surfactant. *J. Agric. Food Chem.* **2004**, *52* (4), 987−91.

(31) Washington, N.; Washington, C.; Wilson, C. G. *Physiological Pharmaceutics: Barriers to Drug Absorption*; Taylor and Francis: London, 2002.